Quaternary Science Reviews 236 (2020) 106293

Contents lists available at ScienceDirect

Quaternary Science Reviews

journal homepage: www.elsevier.com/locate/quascirev

The biogeochemical consequences of late Holocene wildfires in three subalpine lakes from northern Colorado

David P. Pompeani [a, b, *], Kendra K. McLauchlan [a], Barrie V. Chileen [a], W. John Calder [c], Bryan N. Shuman [d], Philip E. Higuera [e]

[a] Department of Geography and Geospatial Sciences, Kansas State University, Manhattan, KS, 66506, USA
[b] Department of Geology, Kansas State University, Manhattan, KS, 66506, USA
[c] Department of Botany, University of Wyoming, Laramie, WY, 82071, USA
[d] Department of Geology and Geophysics, University of Wyoming, Laramie, WY, 82071, USA
[e] Department of Ecosystem and Conservation Sciences, University of Montana, Missoula, MT, 59812, USA

ARTICLE INFO

Article history:
Received 14 November 2019
Received in revised form
25 March 2020
Accepted 31 March 2020
Available online xxx

Keywords:
Fire
Carbon
Nitrogen
Isotopes
Soil
Rocky mountains

ABSTRACT

Wildfire activity has been increasing in forests of western North America over the past several decades. However, the biogeochemical effects of changing fire regimes are poorly understood. Here, we utilize sediment records from three subalpine lakes in northern Colorado (Hinman, Gold Creek, and Summit) to investigate the biogeochemical consequences of charcoal-inferred fire events over the past ~2500 years. We measured element concentrations and stable isotope ratios ($\delta^{13}C$, $\delta^{15}N$) in lake sediments to track past biogeochemical processes. On average, fires were followed by increases in carbon (C), nitrogen (N), and sulfur concentrations in lake sediments, which lasted ~20 years, while titanium and other metals found in terrestrial mineral material decreased. These changes were only statistically significant ($p < 0.10$) for nitrogen, titanium, and $\delta^{13}C$ at Gold Creek Lake, and for sulfur and $\delta^{15}N$ at Hinman Lake, suggesting either that the biogeochemical response to fire is variable through time or that the low temporal resolution of the proxy records (i.e., ~19.2 years/sample) limited the ability to detect short-term impacts. Measurements of C/N, $\delta^{13}C$, and $\delta^{15}N$ suggest that the sources of post-fire C and N differed among the study lakes. Sources of sedimentary organic matter include both erosion of soil organic matter and increased in-lake primary productivity, depending on site-specific watershed characteristics (e.g., vegetation, hydrology, elevation). These results suggest that if fire frequencies increase in the future, soil C and N stocks may not have adequate time to recover after fires, potentially jeopardizing the long-term biogeochemical resilience of these ecosystems.

1. Introduction

Wildfires influence the cycling of carbon (C), nitrogen (N), and other biologically important elements in forested ecosystems (Pellegrini et al., 2018; Schlesinger et al., 2016). Fires volatilize C and N in soils and vegetation, releasing C and N to the atmosphere and reducing terrestrial stocks (Certini, 2005; Smithwick et al., 2005; Yelenik et al., 2013). Wildfire-induced biogeochemical change is also affected by erosional and hydrological loss (Vieira et al., 2018) and subsequent changes in chemical, physical, and biological properties of soils (Alcañiz et al., 2018; Santin and Doerr, 2016). Recent increases in wildfire activity across western North America (Box et al., 2019; Westerling, 2016) have raised questions about potential biogeochemical feedbacks between changing fire regimes and the availability of growth-limiting nutrients in soils (Dunnette et al., 2014; Hudiburg et al., 2017; Leys et al., 2016; Smithwick et al., 2009). Whether forests remain C sinks or become sources depends strongly on the frequency, spatial extent, and severity of future fires (Chapin et al., 2006; Hudiburg et al., 2017; Kelly et al., 2016; Walker et al., 2019).

Multiple studies in coniferous forests indicate that fires can reduce concentrations and stocks of C, N, and other elements in soils (Smithwick et al., 2005), with a least one study suggesting reductions for up to 65 years (Pellegrini et al., 2018). Following a fire, C and N begin to re-accumulate in the soil through microbial

* Corresponding author. Department of Geography and Geospatial Sciences, Kansas State University, Manhattan, KS, 66506, USA.
E-mail address: dpompeani@ksu.edu (D.P. Pompeani).

https://doi.org/10.1016/j.quascirev.2020.106293
0277-3791/

activity and plant regrowth (Dzwonko et al., 2015; Petticrew et al., 2006; Spencer et al., 2003; Turner et al., 2019b; Vieira et al., 2018). However following particularly severe fire events, the large reduction in soil C concentrations may take decades to centuries to recover, creating important legacy effects (Johnstone et al., 2010; Mack et al., 2011; Pompeani et al., 2018; Turner et al., 2019a; Walker et al., 2019). In addition, modeling results suggest soil C stocks can be reduced by up to 13 Mg C ha^{-1} during periods of higher fire frequency or severity, with net C loss lasting nearly 800 years (Hudiburg et al., 2017). In the Alaskan boreal forests, the recent rise in fire frequency inferred from paleorecords led to an estimated loss of 14 Mg C ha^{-1} from 1950 to 2006 (Kelly et al., 2016). Ultimately, the cumulative effect of multiple fire events on soil nutrient availability is an important factor determining biogeochemical resilience – if and how forest ecosystem recover to pre-fire conditions (McLauchlan et al., 2014; Smithwick, 2011). Anticipating the consequences of changing fire regimes under future climate projections is currently limited by the lack of long-term environmental data that document the response and recovery of forest ecosystems to fire events through time.

Lacustrine sediments can provide a long-term perspective on the biogeochemical impact of forest fires. High-severity wildfires emit charcoal particles into the atmosphere, and peaks in macroscopic charcoal (e.g., >125 μm) can be used to infer when fires burned near a lake (Higuera et al., 2010). Several decades of work interpreting sedimentary charcoal concentrations have led to robust methodologies for reconstructing the timing of past wildfire events (Clark, 1988; Higuera et al., 2007; Whitlock and Anderson, 2003). In particular, a network of lacustrine fire records in the western U.S. suggest that fire regimes varied spatially and temporally over the past 3000 years, in response to variations in climate (Calder et al., 2015; Carter et al., 2018; Marlon et al., 2012). Charcoal-based reconstructions from lake sediments can therefore be combined with isotopic and elemental proxies to document the biogeochemical impact of past fires and varying fire regimes.

Few studies have analyzed both biogeochemical proxies and charcoal concentrations to understand differences among atmospheric, erosional, and hydrologic loss pathways after fire, as measured in sedimentary records. For example, at Chickaree Lake in Rocky Mountain National Park, Colorado, concentrations of C, N, and sulfur (S) decreased in sediments deposited 20–50 years following fire events over the past 4200 years (Dunnette et al., 2014; Leys et al., 2016). The interpretation was that C, N, and S held in vegetation and soil volatilized during combustion and were therefore not delivered to sediments, although erosion of mineral materials after fires could have diluted the concentration of organic components in lake sediments. Inorganic elements – titanium (Ti), calcium (Ca), potassium (K), aluminum (Al), and phosphorus (P) – increased significantly in sediments for 15–30 years post-fire, indicating heightened erosional processes after high-severity fire events (Leys et al., 2016). Comparisons of burned and unburned watersheds have shown that fires can increase the transport of C, N, and P in streams for several years following a fire (Spencer et al., 2003). However, this transport is affected by fire intensity (Rhoades et al., 2018) and erosional processes controlled by rainfall and ground cover (Vieira et al., 2018). In addition, the relationships among fire, erosion, and vegetation vary over time, depending on factors including season of burn, fire intensity, time since the last fire, topography, and post-fire biophysical changes (Haliuc et al., 2016). Most of these studies are limited to one or two study sites, or one recent historical fire event. Biogeochemical analyses of lake sediments from a network of sites can be used to compare the effects of multiple fires in the same watershed and across watersheds, over millennia, to reveal how impacts vary as a consequence of variations in dominant controls, such as climate, vegetation type, and geological setting.

Here, we utilize previously-developed charcoal-based fire reconstructions (Calder et al., 2015) from lake-sediment records in northern Colorado, U.S.A., to investigate the biogeochemical impact of wildfire events over the past ~2500 years. We analyzed $\delta^{13}C$, $\delta^{15}N$, and concentrations of nine elements in sediment cores from three subalpine lakes: Hinman, Gold Creek, and Summit. We interpret patterns of variation in elemental concentration of lake sediments at two timescales: we use principal component analysis to characterize dominant modes of variability in the proxies of biogeochemical change over millennial time scales, and we use a compositing analysis to assess the average, decadal-scale biogeochemical response to reconstructed fire events. We then compare the biogeochemical records with previously developed palynological and paleoclimate records to examine potential factors causing similarities or differences in lake response to fire. Results from these comparisons provide perspective on how wildfires affect aquatic and terrestrial ecosystems and provide insight into how future changes in fire regimes will impact the biogeochemical resilience of subalpine forests.

2. Materials and methods

2.1. Study area

We utilized existing sediment records from three small subalpine lakes spanning and elevational gradient in the Routt National Forest in northern Colorado, U.S.A. (Calder et al., 2015) (Fig. 1, Table 1): Hinman, Gold Creek, and Summit lakes. Hinman Lake (40.771°, −106.827°; 2501 m asl; 0.03 km^2) has no surficial inflow or outflow streams, a water depth of 10 m, and a low-relief watershed. Bedrock in the catchment consists of Cretaceous clastic sedimentary rocks (Horton et al., 2017) overlain with thin soils and glacial till. The southern part of the catchment is dominated by subalpine fir (*Abies lasiocarpa*) and Engelmann spruce (*Picea engelmannii*), while the northern part of the catchment is covered in shrubs and aspen (*Populus tremuloides*). Gold Creek Lake (40.781°, −106.678°; 2917 m asl; 0.04 km^2) has a depth of 10.6 m, one inflowing and outflowing stream, and is situated in the watershed with the highest topographic relief of the three sites. The watershed is underlain with Precambrian gneiss bedrock (Snyder, 1978) covered with glacial till and shallow soils, and forest composition is dominated by subalpine fir and Engelmann spruce. Hinman and Gold Creek lakes occupy low and middle elevations, respectively, where recent forest history and disturbances have been analyzed using dendroecological techniques (Howe and Baker, 2003). Summit Lake (40.545°, −106.682°; 3149 m asl; 0.02 km^2) is the highest elevation lake and has small inflowing and outflowing streams. The lake is approximately 5.9 m deep with a gently sloping watershed underlain with Precambrian granite and gneiss bedrock (Horton et al., 2017) covered by thin discontinuous soils. Summit Lake is located adjacent to the Continental Divide at the crest of Buffalo Pass, a low point in the broad forested plateau that defines the southern portion of the area. Alternating bands of subalpine fir and Engelmann spruce forest separated by meadows comprise the local vegetation (Calder et al., 2015). Modern climate at the three lakes, as represented by PRISM, spans a gradient in climate, with monthly mean temperatures declining and precipitation increasing with elevation. Temperatures range from −6.5 °C (at Hinman, lowest elevation) to −9.2 °C (at Summit, highest elevation) in January and 15.9 °C–13 °C in July. Average total annual precipitation more than doubles from 672 mm (Hinman) to 1482 mm (Gold Creek) and 1530 mm (Summit). Average January precipitation of 65–186 mm typically is more than double average July precipitation of 34–45 mm, with most precipitation delivered

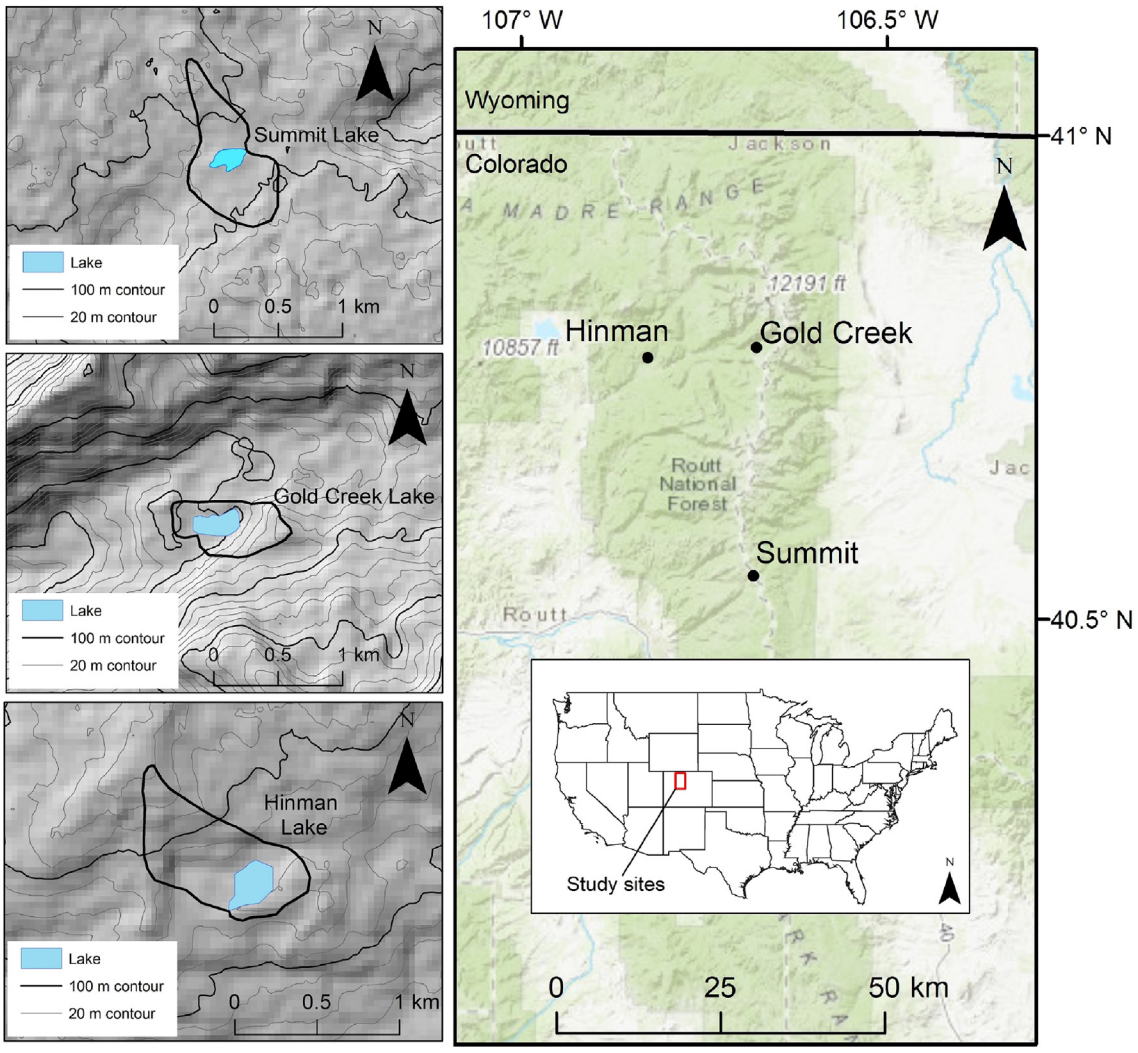

Fig. 1. (Left) Watershed maps ordered from highest (top) to lowest (bottom) elevation. The thick black line indicates the lake watershed boundary. (Right) Regional map of the study lakes.

Table 1
Study site characteristics.

Lake	Surface area (ha)	Watershed area (ha)[a]	Depth (m)	Temp. (C)[b]	Dissolved O_2 (mg/l)[b]	SpC (μs/cm)[b]	pH[b]	NO_3 (mg/l)[b]	Alkalinity (mg/l)
Summit	1.9	49	5.9	11	17	12	7	11	2
Gold Creek	3.7	25	10.6	10	12	49	8	5	7
Hinman	2.7	45	10	11	6	159	7	5	54

[a] Does not include lake surface area.
[b] Average value of the water column.

as snow in the winter months.

2.2. Sediment core collection and chronology

The study lakes were cored between 2010 and 2012, as described by Calder et al. (2015). Cores 80–145 cm in length were obtained from at least 5 m water depth using a polycarbonate tube fitted with a piston. The sediment chronologies for all three lakes were based on a combination of ^{210}Pb activity in 12 samples from the upper 35 cm of sediment and 14 accelerator mass spectrometry ^{14}C dates. The ^{210}Pb chronology was developed using the constant rate of supply model (Binford, 1990). Radiocarbon ages were calibrated relative to 1950 CE (hereafter 'yr BP') using the IntCal13 dataset (Reimer et al., 2013). We used the original published chronologies, which were developed using the Bchron package for R (Haslett and Parnell, 2008; Parnell et al., 2008) (Fig. S1). Bchron models sediment age with a conservative Bayesian framework under the assumption that sedimentation is monotonic, piecewise linear, and continuous (Parnell et al., 2008).

2.3. Modern water chemistry

The water chemistry of the study lakes was measured in July 2018 using a YSI ProPlus multiparameter sonde fitted with

temperature, dissolved oxygen, specific conductivity, pH, and nitrate sensors. Measurements were made in the center of lake at 1-m intervals to the bottom of the lake or to a depth of 10 m (the maximum depth of the probe). Total bicarbonate and carbonate concentrations in surface water were measured in the field via sulfuric acid titrations using a Hach Alkalinity Test Kit.

2.4. Sediment biogeochemistry

A total of 336 sediment samples were analyzed for elemental concentrations (119 at Gold Creek, 82 at Hinman, and 135 at Summit) in the Paleoenvironmental Lab in the Department of Geography and Geospatial Sciences at Kansas State University. Samples 0.5–1.0 cm thick were dried at 80 °C for 48 h and homogenized prior to analysis. We measured the concentration of seven elements (Al, Si, P, S, K, Ca, Ti) using a handheld Bruker Tracer 5i wavelength-dispersive X-ray fluorescence (XRF) analyzer. Major and trace elements were measured consecutively, with sampling spanning 180 s for major elements and 120 s for minor elements. Counts of photons emitted were compared against a soil calibration to calculate concentration (% dry mass). Ten measurements of the soil standard (Bruker CS-M2) were conducted before and after analyzing unknowns to ensure accuracy within acceptable limits. Precision for individual metal concentrations were calculated using repeat measurements of sediment samples made throughout the period of analysis ($n = 102$). Precision values (one relative standard deviation) for metal concentrations were between ± 2–8%.

The concentration and isotopic composition of sediment C and N were measured across continuous samples at an average resolution of 19.2 years per sample, with a total of 113 samples analyzed from the Gold Creek, 80 from Hinman, and 162 from Summit. Sediments were dried at 80 °C for 48 h then homogenized before analysis in a Costech 4010 Elemental Analyzer coupled to a Thermo Finnigan Delta V Plus XP isotope ratio mass spectrometer at the University of Wyoming Stable Isotope Facility. Standardized isotope ratios for C were reported relative to VPDB, and for N relative to N_2 atmospheric gas, both using standard delta notation ($\delta^{13}C$, $\delta^{15}N$) and units of per mil (‰). Analytical precision was based on repeated measurements. Precision for %C and %N was ±3.5%; precision for $\delta^{13}C$ and $\delta^{15}N$ was ±0.5‰ and ±1.8‰, respectively.

2.5. Wildfire history

The largest wildfire in the study area over the observational record occurred in 2002, when 12,648 ha of forest burned in the Mount Zirkel Wilderness. While Gold Creek and Hinman lakes are located close to this fire (i.e., within 1.75–3 km), only a small portion of the watershed of Gold Creek Lake was burned in the 2002 fire; Summit Lake is located ~15 km south of the area burned. Consequently, and because it was downwind of much of the area burned, Gold Creek Lake has the highest amount of charcoal in the 21st century sediments (Calder et al., 2015). Beyond the observational record, fire history at each lake was based on continuous samples of macroscopic charcoal concentrations converted to charcoal accumulation rates (CHAR), as described by Calder et al. (2015). Theoretical and empirical evidence suggests that distinct peaks in charcoal from lake sediments represent fires occurring within approximately 1 km of small (e.g., ~0.1 km^2) lakes (Higuera et al., 2010). Wet sediment samples (1–4 cm^3) were oxidized in sodium hypochlorite (Gold Creek and Hinman Lakes) or 6% hydrogen peroxide (Summit Lake) and sieved at 125 μm, isolating charcoal pieces that were counted under a stereomicroscope. Statistically significant peaks in charcoal concentrations were identified using the *CharAnalysis* program (Higuera et al., 2009), as described by Calder et al. (2015). Significant CHAR peaks are hereafter referred to as fire events. Calder et al. (2015) inferred 33 high-severity fire events among all three lakes. The average (±standard deviation) return interval between fire events was 123 ± 49 years at Hinman Lake, 183 ± 110 years at Gold Creek Lake, and 198 ± 109 years at Summit Lake for the respective length of each sediment record (Calder et al., 2015).

2.6. Statistical analysis

We conducted principle component analyses (PCA) in MATLAB to summarize the dominant modes of variation in the records of elemental concentrations and isotopic values. Prior to analysis, all series in all three records were linearly interpolated to 20-year resolution and standardized with respect to mean and standard deviation (i.e., z-scores).

We assessed the biogeochemical impacts of fire events using a compositing technique, similar in concept to superposed epoch analysis. The age of the fire events identified in *CharAnalysis* are slightly offset from the actual age of the charcoal peak in the raw record, as a result of the uniform temporal interpolation done in the program. Thus, the timing of the fire events was refined to correspond to the more precise timing of the peak in charcoal concentration in the uninterpolated data (see Table S1). For each charcoal peak, the measurements of each element or isotope before, coincident with, and after the fire event were identified. The three measurements were then standardized using z-scores. The response series was calculated by averaging the z-scores from across all fires within a single record, and these response series were plotted as boxplots. A non-parametric analysis of variance (Kruskal-Wallis test) was used to test the null hypothesis that the samples did not differ among the three populations of z-scores (i.e., before, during, and after fire events). We considered the populations different if the resulting p-value was <0.10 (see Figs. S2-S4).

3. Results and discussion

3.1. Modern water chemistry

The surface water in all three lakes was characterized by low alkalinity (2–54 mg/l) (Table 1). Dissolved oxygen and specific conductivity measurements indicated that the lake water columns were poorly stratified. However, at Hinman Lake the hypolimnion was anoxic (<1 mg/l). Nitrate concentrations in all three lakes ranged from 1 to 19 mg/l and pH was between 6.3 and 8.6. The water in Hinman Lake contained the highest specific conductivity values on average (Table 1), likely reflecting underlying sedimentary bedrock that contributes to higher solute loads to groundwater, relative to the resistant igneous and metamorphic bedrock underlying Gold Creek and Summit lakes. In general, these analyses suggest that the study lakes contain soft water (Briggs and Ficke, 1977) and are poorly buffered (Michelutti et al., 2006).

3.2. Past variations in elemental concentrations

At Hinman Lake, Ti, Si, K, Ca, and Al concentrations fluctuated a small amount on multi-decadal timescales (Fig. 2). S, C, and N concentrations exhibited high amplitude shifts early in the record, which decreased in amplitude after 900 yr BP, until C and N increased during the 20th century. P concentrations remain at low and stable values, except for a distinct increase from 700 to 900 yr BP. Similarly, at Gold Creek Lake, Ti, Si, K, Ca, and Al concentrations varied slightly on multi-century timescales for the duration of the 2000-yr sedimentary record. S, P, C, and N concentrations decreased ~900 yr BP, followed by a gradual and steady increase in

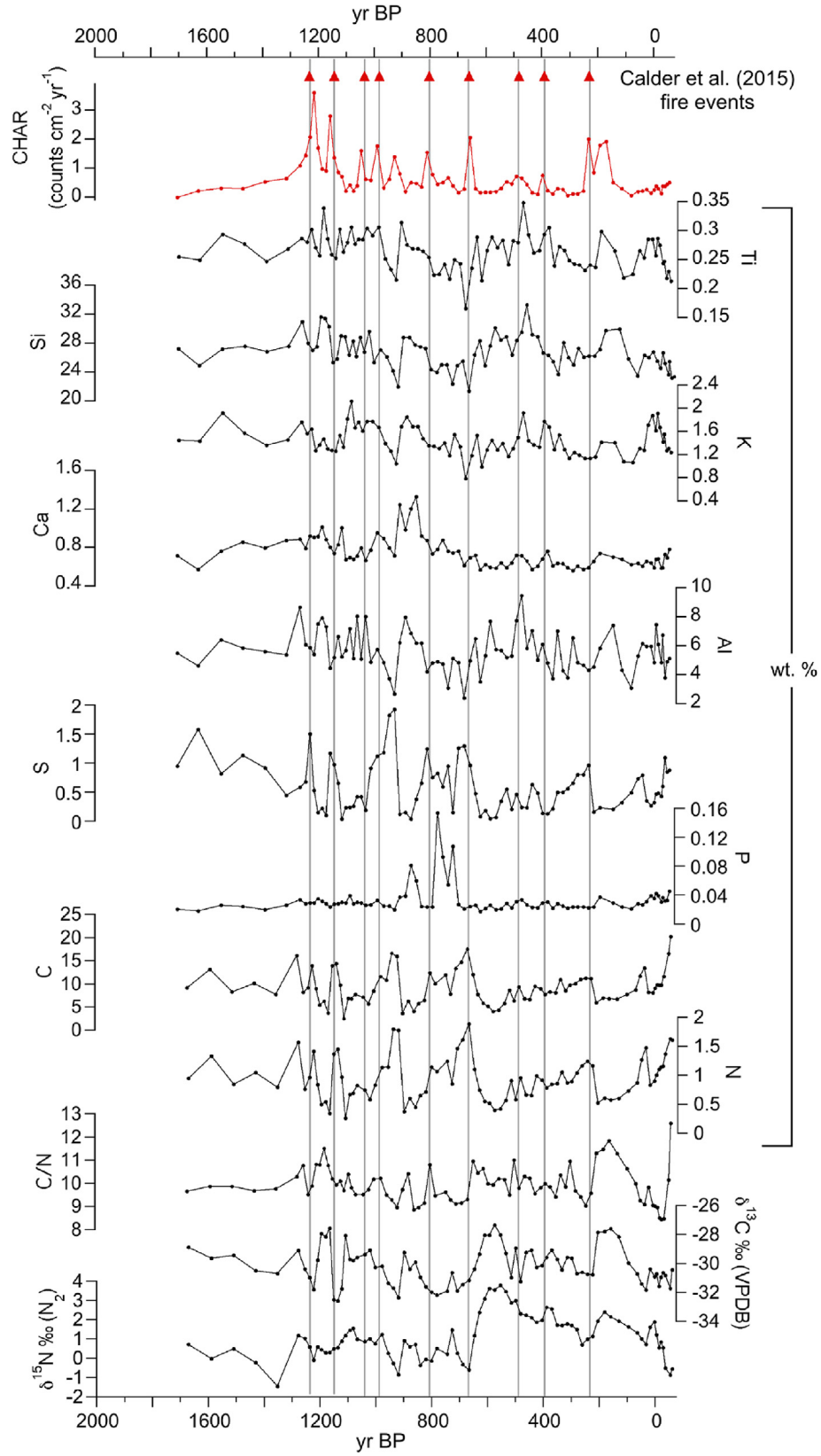

Fig. 2. Elemental concentrations, $\delta^{13}C$, and $\delta^{15}N$ proxies from sediment in Hinman Lake, Colorado, U.S.A. Triangles indicate previously identified fire events from Calder et al. (2015).

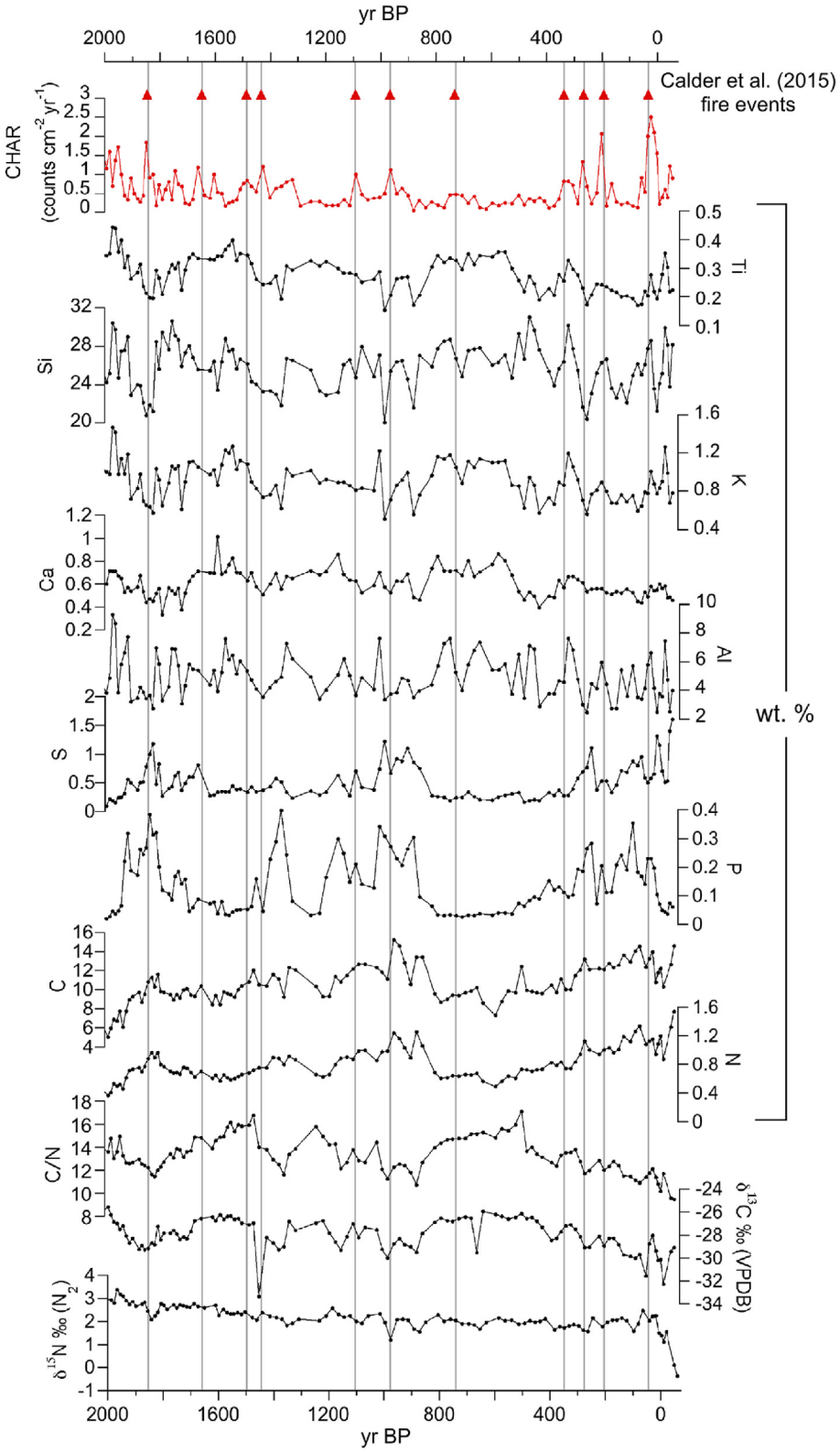

Fig. 3. Elemental concentrations, $\delta^{13}C$, and $\delta^{15}N$ proxies from sediment in Gold Creek Lake, Colorado, U.S.A. Triangles indicate previously identified fire events from Calder et al. (2015). (For interpretation of the references to colour in this figure legend, the reader is referred to the Web version of this article.)

percentages until the 20th century (Fig. 3). At Summit Lake, Ti, Si, K, Ca, and Al displayed highly variable concentrations on multi-decadal timescales until abrupt increases in the 20th century. P and N concentrations remained relatively low until the 20th century increase. C and S concentrations are highest prior to 2000 yr BP and slowly declined until the 20th century (Fig. 4).

The relatively high average concentrations of S, K, and Ca in Hinman Lake sediments (Table 2) were attributed to the relatively

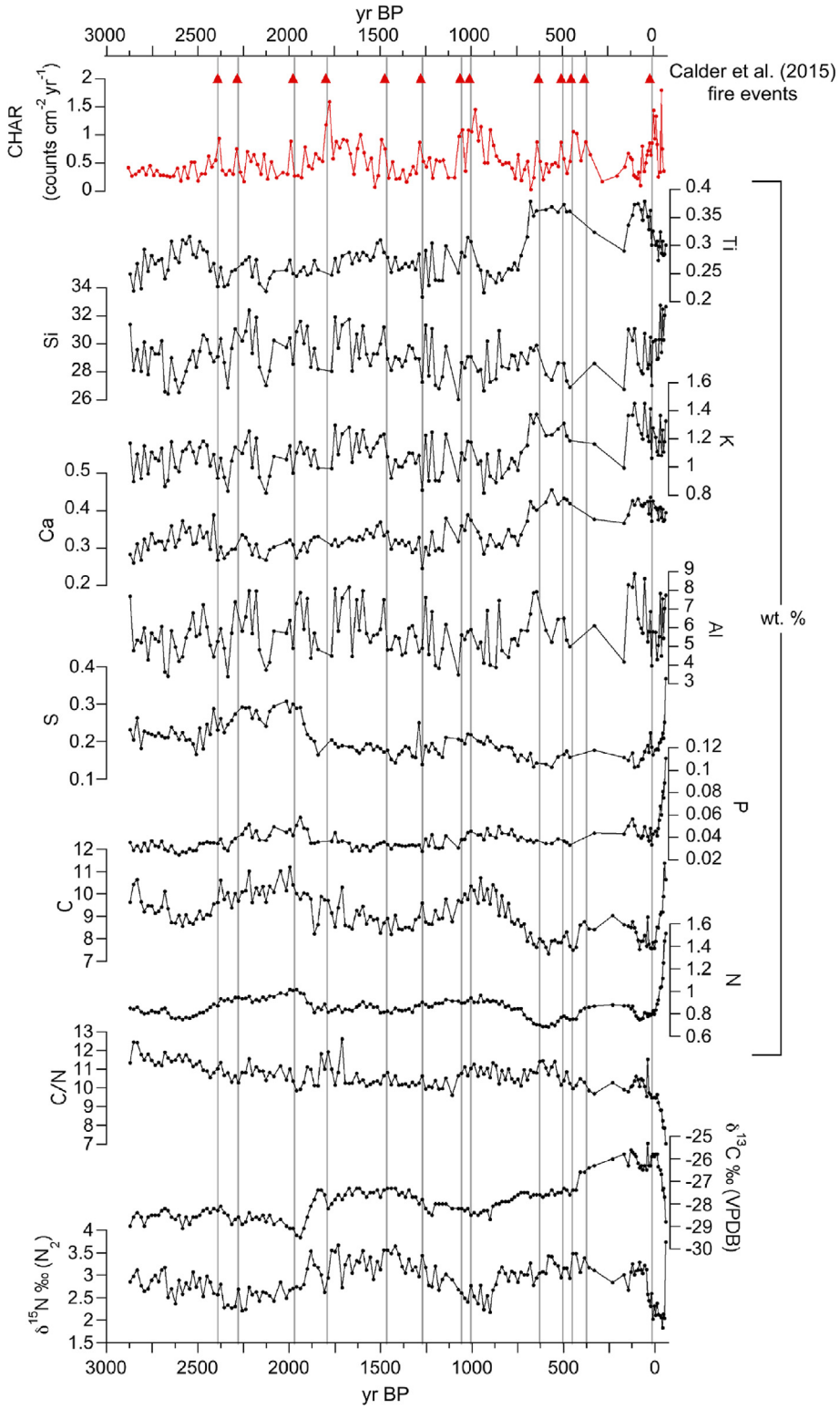

Fig. 4. Elemental concentrations, $\delta^{13}C$, and $\delta^{15}N$ proxies from sediment in Summit Lake, Colorado, U.S.A. Triangles indicate previously identified fire events from (Calder et al., 2015).

unique bedrock composition of the watershed compared with Summit Lake and Gold Creek Lake. Hinman Lake is underlain with sedimentary bedrock, which is more susceptible to physical and chemical weathering, relative to the resistant igneous and metamorphic rocks underlying Gold Creek and Summit lakes (Horton et al., 2017; Snyder, 1978). As a consequence of these bedrock differences, solute loads were higher in the water of Hinman Lake (Table 1), leading to higher percentages of S, K, and Ca in the sediment.

Table 2
Average proxy values across the duration of the record.

Lake	Resolution[a] (yr/sample)	Ti (%)	Si (%)	S (%)	P (%)	K (%)	Ca (%)	Al (%)	$\delta^{15}N$ (‰)	$\delta^{13}C$ (‰)	C (%)	N (%)	C/N
Summit	19	0.3	29	0.2	0.04	1.1	0.3	5.8	2.9	−27.8	9.1	0.9	10.6
Gold Creek	19	0.3	26	0.5	0.13	0.9	0.6	5.0	2.2	−27.9	10.5	0.8	13.3
Hinman	22	0.3	27	0.6	0.03	1.4	0.7	5.6	1.1	−30.1	9.2	0.9	9.9

[a] Average resolution of the element and isotope proxies.

3.3. Past variation in $\delta^{13}C$, $\delta^{15}N$, and C/N

The average sedimentary $\delta^{13}C$ values in Hinman, Gold Creek, and Summit lakes (Table 2) were around −27‰, consistent with previously reported averages for lacustrine organic matter produced by algae (assuming surface water in isotopic equilibrium with atmospheric CO_2) and in land plants using the C3 pathway (Meyers, 1997) (Figs. 2–4). Average $\delta^{15}N$ values were between 1.1 and 2.9‰, which is within the range of natural values reported in organic matter for sediments from freshwater lakes and wetlands (Elliott and Brush, 2006). Organic matter in Gold Creek Lake contrasts with that from Summit and Hinman lakes in that it had higher average C/N ratios (Table 2), suggesting that Gold Creek Lake receives a greater proportion of C-rich terrestrial organic matter (Meyers, 1997), likely because the stream inflow efficiently transports watershed-derived organic matter into the lake.

The trends in C/N, $\delta^{13}C$, and $\delta^{15}N$ at each lake were distinct (Figs. 2–4). Hinman Lake, which has no input or outflow stream, experienced the greatest variation in these three measurements. C/N and $\delta^{13}C$ varied on centennial scales, and $\delta^{15}N$ experienced a positive shift at ca. 600 yr BP (Fig. 2). In contrast, $\delta^{15}N$ values at Gold Creek Lake only experienced a small negative trend of <1‰ before the 20th century, and C/N and $\delta^{13}C$ record low amplitude, multi-century variations with trends to their minima over the past 500 years (Fig. 3). Summit Lake reveals another distinct set of long-term trends with little change in C/N, but a gradual increase in $\delta^{13}C$ (Fig. 4). Prior to the 20th century, $\delta^{15}N$ values at Summit Lake experienced modest multi-century variations (Fig. 4).

3.4. Principal component analysis of biogeochemical proxies and interpretation of sediment origin

Results of the lake-specific PCAs using sedimentary elemental concentrations (C, N, S, P, Ca, K, Al, Ti, Si, C/N) and stable isotopes ($\delta^{13}C$, $\delta^{15}N$) revealed two modes of variability in the biogeochemical variables (Fig. 5). In general, the first principal component was associated with organic matter (e.g., C, N, S, etc.), while the second principal component was positively correlated with elements found in mineral material (Al, K, Si, Ca, etc.). The distribution of stable isotopes and C/N along the first and second principal component axis varied by lake, depending on the source (i.e., autochthonous versus allochthonous) and amount of organic material.

At Hinman Lake, PC 1 and 2 explained 43.2% and 20.2% of the total variation in the proxies, respectively (Fig. 5). C, N, and S were positively correlated with PC 1, and Si, $\delta^{13}C$, Al, Ti, and C/N were negatively correlated with PC 1 (Table 3). The high positive loadings of C and N on PC 1 suggest that variation in the proxies was driven by changes in organic matter concentrations. Specifically, increased C and N concentrations correspond with declines in C/N values, suggesting that variation in organic matter was driven by a

Table 3
Principal component eigenvalues.

Proxy	Summit Lake		Gold Creek Lake		Hinman Lake	
	PC 1 45%	PC 2 23%	PC 1 58%	PC 2 11%	PC 1 43%	PC 2 20%
Ti	0.42	0.07	0.35	0.06	−0.33	0.31
Si	−0.02	0.57	0.23	0.47	−0.37	0.16
S	−0.34	0.26	−0.29	0.17	0.32	0.15
P	0.01	0.31	−0.28	0.01	0.03	0.19
K	0.35	0.37	0.33	0.32	−0.20	0.45
Ca	0.40	0.02	0.26	0.09	−0.05	0.48
Al	0.17	0.53	0.25	0.53	−0.33	0.32
$\delta^{15}N$	0.23	−0.13	0.18	−0.33	−0.26	−0.38
$\delta^{13}C$	0.34	−0.09	0.30	−0.11	−0.33	−0.24
N	−0.25	0.19	−0.34	0.31	0.37	0.15
C	−0.40	0.16	−0.29	0.33	0.35	0.13
C/N	−0.14	−0.08	0.31	−0.15	−0.25	−0.21

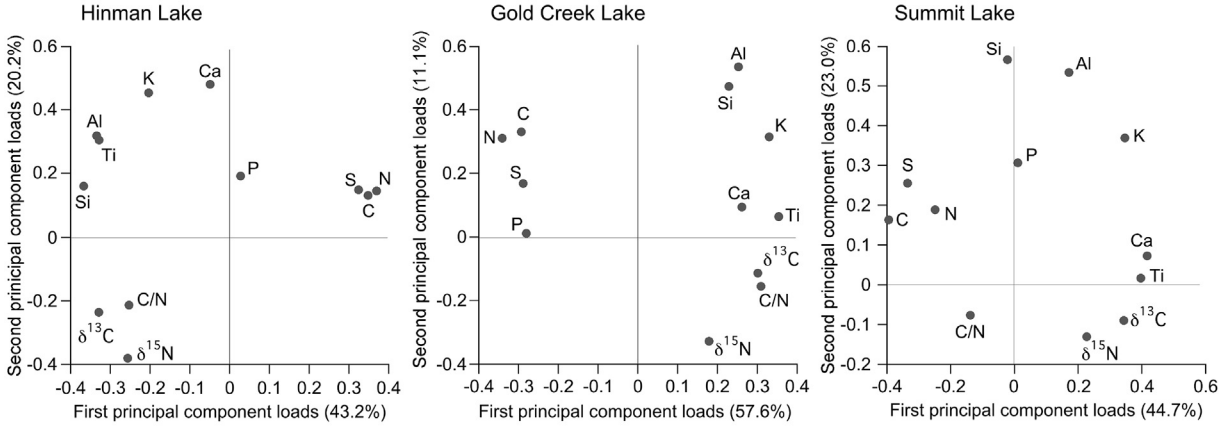

Fig. 5. Proxy principal component loads for the study lakes. Principal component analyses reveal two primary groupings: (1) proxies associated with organic matter (C, N, S) and (2) elements found in mineral material (Ti, Ca, K, Al). Depending on the study lake, P is associated with either organic matter or mineral proxies (or some mixture). This is attributed to whether P is found in a mineral form (i.e., bedrock source) or as occluded/organic P (i.e., bound to soil oxides and/or associated with the remains of plants) in the sediments (Filippelli et al., 2009).

combination of algal productivity and terrestrial organic matter. Increased Si, Ti, Al, and C/N values correspond to declines in C and N concentrations. P values generally fell along the middle of PC 1 and was more positively loaded on the PC 2 axis (Fig. 5). The weak association of P with C, N, and C/N implies that P was not strongly linked to higher organic matter concentrations, suggesting instead that P is found in the sediment as a mixture of mineral and organic matter forms (Filippelli et al., 2009).

At Gold Creek Lake, PC 1 and 2 explained 57.6% and 11.1% of the total variability in the record, respectively (Fig. 5). PC 1 was positively correlated with Ti, K, C/N, $\delta^{13}C$, and Ca, and negatively correlated with N, C, S, and P. PC 2 was positively correlated with Ti, Si, and K, and negatively correlated with $\delta^{15}N$ and C/N (Table 3). The high positive loadings of Ti, K, C/N, $\delta^{13}C$, and Ca on PC 1 suggest that the dominant mode of variation in the proxies was driven by fluctuations in terrestrially-sourced organic matter and mineral concentrations. In turn, lower PC 1 scores were associated with higher concentrations of C, N, S, P, and lower C/N values. P was negatively correlated with PC 1, similar to C, N, and S, suggesting that P was associated with organic matter (Filippelli et al., 2009). Since P commonly limits primary productivity in lakes (Bracken et al., 2015; Schindler et al., 2016), increased P in the sediment may reflect periods of greater in-lake productivity. This interpretation is supported by PC 2, where sediment samples with lower C/N and $\delta^{15}N$ values also have higher C and N values.

At Summit Lake, PC 1 and 2 explained 44.7% and 23.0% of the total variation in the proxies, respectively (Fig. 5). Ti, Ca, K, and $\delta^{13}C$ were positively loaded on PC 1, with C, S, N, and C/N negatively loaded. PC 2 was positively correlated with Si, Al, and P, and negatively correlated with $\delta^{15}N$, $\delta^{13}C$, and C/N (Table 3). PCA suggests that the primary mode of variation at Summit Lake was caused by fluctuating concentrations of Ti and Ca, with relative declines in C and N. The negative relationship between Si and P versus $\delta^{15}N$, $\delta^{13}C$, and C/N, highlighted by PC 2, suggests that higher values along PC 2 were associated with relatively higher amounts of algal-derived organic matter.

3.5. Biogeochemical responses to fire events

The composite analysis of the biogeochemical proxies at all three lakes revealed that sediments deposited during and immediately following fire events had modestly higher average organic matter (i.e., C, N, and S) concentrations and lower concentrations of Ti and other inorganic elements. However, these changes were only statistically significant ($p < 0.10$) for N, Ti, and $\delta^{13}C$ at Gold Creek Lake, and for S and $\delta^{15}N$ at Hinman Lake (Fig. 6). This suggests either a minimal or muted biogeochemical response to fires for the few reconstructed fire events ($\leq$13), or that the temporal resolution of the proxy records (i.e., ~19.2 years/sample) is too coarse to detect possible short-term responses to fire events (Morris et al., 2015). In general, we attribute higher average organic matter concentrations following fires to some mix of terrestrial sources and increased aquatic primary productivity, while Ti and other inorganic elements decline, likely as a result of dilution with organic material.

Values of $\delta^{13}C$, $\delta^{15}N$, and C/N ratios indicate that the source of fire-related sedimentary organic matter was different at each study lake (Fig. 6). For example, at Gold Creek Lake, post-fire decreases in C/N and increases in $\delta^{13}C$ suggest that the rise in fire-related organic matter was driven primarily by in-lake productivity (Meyers, 1997), possibly as a result of nutrient releases in ash. Gold Creek Lake has a surface inflow, allowing soluble P released in ash (Cade-Menun et al., 2000; Certini, 2005) to be efficiently delivered to the lake (Fig. 5a). High N and P loads in streams following a fire have been documented in montane ecosystems in Glacier National Park, Montana (Spencer et al., 2003). Because N and P are commonly limiting nutrients in aquatic ecosystems (Bracken et al., 2015), the transport of nutrients following a fire would likely promote aquatic primary productivity. At Hinman Lake, post-fire increases in C/N and decreases in $\delta^{13}C$ values suggest a mix of C and N from terrestrial sources and increased aquatic primary productivity following fires (Fig. 6). However, at Summit Lake, the highest of the three study sites, higher sediment C/N, $\delta^{13}C$, and $\delta^{15}N$ values during fires indicate a predominantly terrestrial organic matter source (Fig. 6) (Meyers, 1997). Thus, differences in organic matter source are attributed to local conditions (e.g., climate, elevation, hydrology, vegetation) at each lake (Dunnette et al., 2014; Leys et al., 2016).

3.6. Long-term patterns of biogeochemical change

The biogeochemical patterns in the Hinman, Gold Creek, and Summit lake sedimentary records feature millennial-scale trends that provide important context for ongoing environmental changes in subalpine forests. We use PC 1 from each site to characterize the dominant mode of variation in the proxy records through time (Figs. 5 and 7). PC 1 at Summit Lake increases over the last ~2900 years, particularly after 1000 yr BP, suggesting a shift to higher concentrations of mineral matter (e.g., Ti, Ca, and K). At Gold Creek Lake, PC 1 declines over the last 2000 years, suggesting a shift to more C- and N-dominated sediment. At Hinman Lake, the shortest record, PC 1 varies on centennial timescales but does not have a long-term overall trend (Fig. 7).

There are several potential interpretations for disparate trends in the proxies characterized by PC 1 among the study lakes (Fig. 7). First, the charcoal-based fire reconstructions by Calder et al. (2015) suggest that the frequency of past fires is unique to the areas surrounding each lake. Observational (Adkins et al., 2019) and modeling (Hudiburg et al., 2017) evidence indicates that fire-regime variability is a dominant driver of soil C-dynamics in coniferous forests, with biogeochemical legacies potentially lasting centuries to millennia. If soil C concentrations reflect a unique fire history in each watershed, it could potentially affect delivery of C to the sediments. Second, paleoclimate reconstructions indicate that climate varied over the late Holocene in this region. For example, sediment-based $\delta^{18}O$ proxies record a shift from a rain-dominated to snow-dominated precipitation regime over the last 3000 years at Bison Lake (~200 km southwest) (Anderson, 2011). Changes in winter precipitation inferred from fossil pollen, and recent increases in regional lake levels support the inferred increase in snowfall over the past ~1000 years (Jiménez-Moreno et al., 2019; Parish et al., 2020; Shuman et al., 2009, 2018). Furthermore, reconstructions of the Palmer Drought Severity Index indicate that areas experiencing drought increased from 1050 to 700 yr BP across western North America, transitioning to regionally wetter conditions over the last ~700 years (Cook et al., 2007). However, the importance of these changes may vary with elevation, particularly given the doubling of modern observed precipitation with elevation across our study sites. If so, or if factors like slope, aspect, and vegetation effects on snow drifting influence local soil moisture and runoff history differently among sites, we may expect differences in the climate-driven effects on biogeochemistry. Consistent with a strong effect at the snowiest, high-elevation site (Summit Lake), PC 1 there tracks the $\delta^{18}O$ and pollen-inferred record of the late-Holocene precipitation changes in northern Colorado (see Calder and Shuman (2017) and Parish et al. (2020)).

The varying biogeochemical response among the three study lakes might also reflect lake-specific shifts in vegetation composition due to climate change. For example, widespread fires and transition to snow-dominated precipitation around 1000 yr BP led to the development of ribbon forests (i.e., linear bands of forest

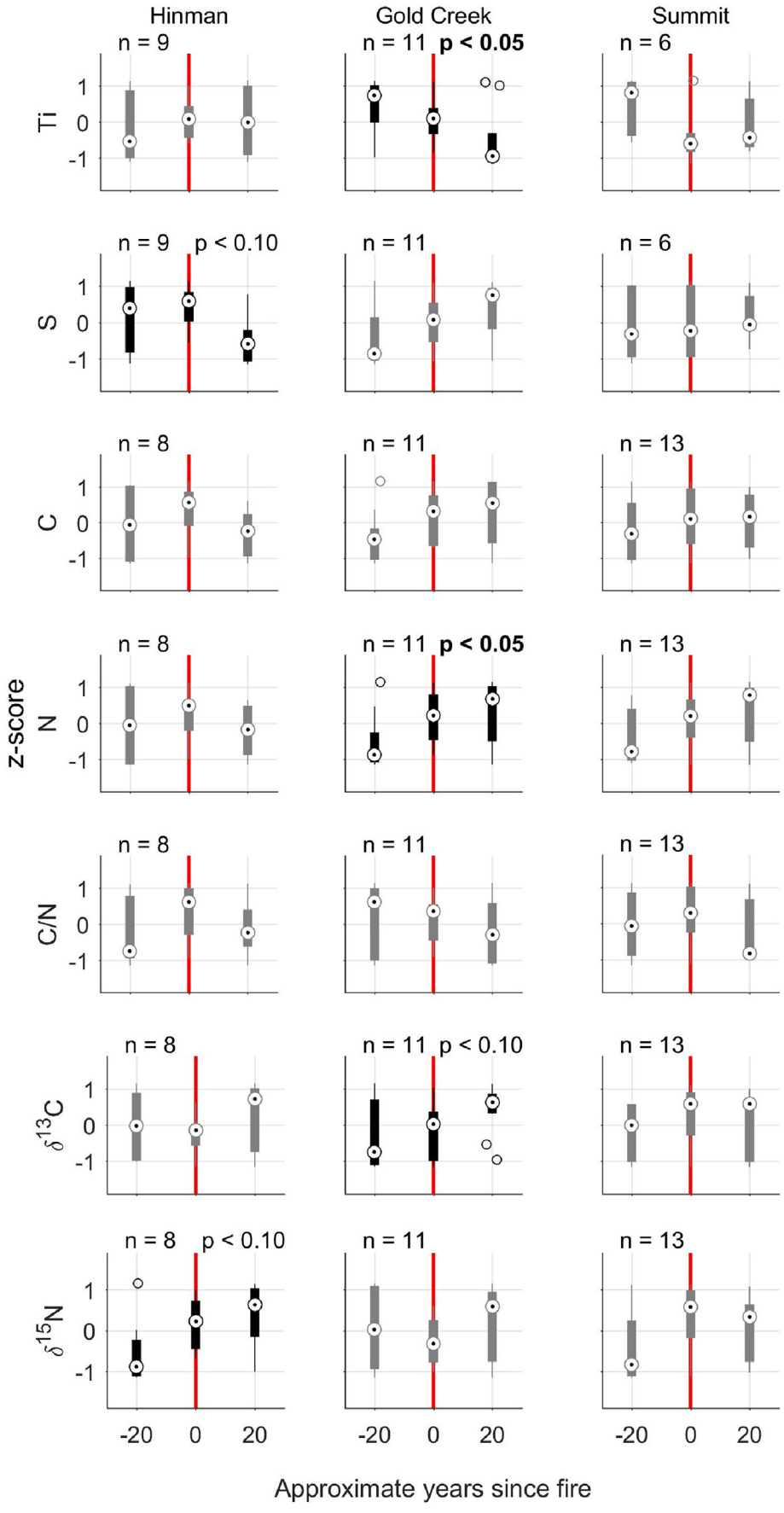
Hinman
Gold Creek
Summit
n = 9
n = 11 p < 0.05
n = 6
n = 9 p < 0.10
n = 11
n = 6
n = 8
n = 11
n = 13
n = 8
n = 11 p < 0.05
n = 13
n = 8
n = 11
n = 13
n = 8
n = 11 p < 0.10
n = 13
n = 8 p < 0.10
n = 11
n = 13
Ti
S
C
N
C/N
δ13C
δ15N
z-score
1
0
-1
-20
0
20
Approximate years since fire

Fig. 6. Composite patterns of selected proxies before, during, and after fire events from Summit, Gold Creek, and Hinman lakes. Boxes enclose the 25, 50th (median, double-circle symbol) and 75th percentiles, whiskers extend to the 10th and 90th percentiles, and single circles illustrate outliers. Proxies with significant differences among pre-, during-, and post-fire populations are shown in bold, with the p-value range from the Kruskal-Wallis non-parametric ANOVA noted. The median time between samples before and after a fire events ranged from 18 to 20 years; thus, the x-axis represents an approximate time since fire. (For interpretation of the references to colour in this figure legend, the reader is referred to the Web version of this article.)

separated by meadows of herbaceous flora) near Summit and Gold Creek lakes, but not at Hinman Lake, which experienced a shift to more open mid-elevation aspen-fir (*Populus tremuloides-Abies lasiocarpa)* forests (Calder et al., 2015, 2018). In the case of Summit Lake (Fig. 4), the development of ribbon forests likely reduced overall biomass production in the watershed, thereby reducing the input of terrigenous organic matter to the lake sediments. However, at Hinman and Gold Creek lakes, the widespread fires and regional shift to snow-dominated precipitation around 1000 yr BP do not appear to have reduced terrestrial (or aquatic) productivity, as reflected in sedimentary C and N concentrations (Figs. 2 and 3) and pollen reconstructions (Calder et al., 2018).

4. Conclusions and implications for biogeochemical resilience to wildfires

This study provides an important early step toward integrating the complex effects of fire on lakes, which currently limits our ability to predict responses across varying fire regimes, lakes, and watersheds (McCullough et al., 2019). Our results indicate that fire events during the past ~2500 years caused a relatively brief (~20 year) increase in sedimentary C, N, and S concentrations, and a decline in Ti and other elements associated with mineral matter (Fig. 6). However, the statistical significance of these changes was different among lakes and proxies, suggesting variable biogeochemical responses to variable fire events, or that the temporal resolution of the proxy records (i.e., ~19.2 years/sample) is too coarse to detect what may be short-term impacts of fire events (Morris et al., 2015). This highlights the important need for high-resolution analysis (<10 years/sample) to study the biogeochemical impact of fires using lake-sediment records. The primary mechanisms for increasing organic matter concentrations at Hinman and Summit lakes are attributed to the erosion of soils into the lake and secondary increases in primary productivity. At Gold Creek Lake, the release of nutrients in the watershed as a result of fire appears to have promoted in-lake primary productivity, increasing the concentrations of organic matter with lower C/N values, consistent with another subalpine watershed in the region (Dunnette et al., 2014). These multi-decadal shifts are superimposed on millennial-scale trends in proxy values related to climate and vegetation change, as reflected in PC 1 (Fig. 7). The repeated recovery of vegetation (Calder et al., 2018) and biogeochemical proxies (here, and in nearby Rocky Mountain National Park, Dunnette et al. (2014)) over the late Holocene implies an inherent biogeochemical resilience of subalpine forest in the region to fire. If predicted warmer and drier summers (Ray et al., 2008) increase fire frequency and/or severity, and particularly if return intervals decrease to multi-decadal timescales, this long-standing resilience may become compromised (Turner et al., 2019a). Further characterization of the feedbacks between forest biogeochemistry and fire-regime variability will improve predictions of ecosystem function under scenarios of future climate change.

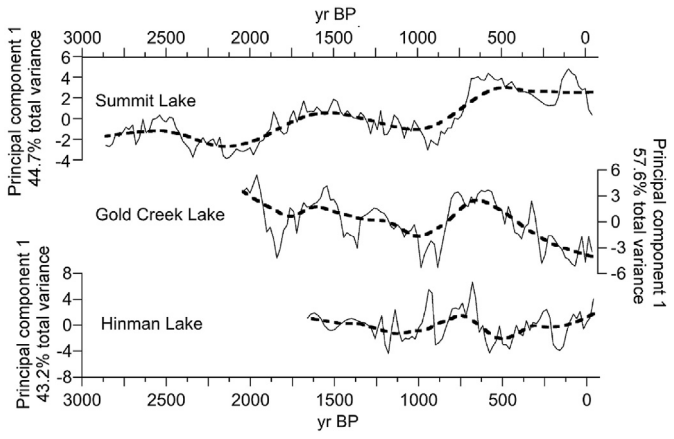

Fig. 7. Principal component 1 (from Fig. 5), used to characterize low frequency trends in the proxy data. Black dotted line is the smoothed lowess curve, representing millennial-scale trends.

Data availability

All data are archived online at the NOAA Paleoclimatology Database.

Author Statement

David P. Pompeani: conceptualization, XRF analysis, writing, MATLAB code. Kendra K. McLauchlan: conceptualization, writing. Barrie V. Chileen: code writing. W. John Calder: pollen and charcoal analysis. Bryan N. Shuman: pollen and charcoal analysis, editing. Philip E. Higuera: MATLAB code, charcoal analysis, editing.

Declaration of interests

The authors declare that they have no known competing financial interests or personal relationships that could have appeared to influence the work reported in this paper.

Acknowledgements

This work was supported by National Science Foundation (NSF) awards DEB-1655179 to KKM, DEB-1655189 to BNS, and DEB-1655121 to PEH. DPP was supported by NSF award DEB-1145815. J. Roozeboom provided analytical assistance. We thank other Big Burns team members T. Hudiburg, K. Bartowitz, K. Wolf, and M. Hastings for field assistance and valuable discussions.

Appendix A. Supplementary data

Supplementary data to this article can be found online at https://doi.org/10.1016/j.quascirev.2020.106293.

References

Adkins, J., Sanderman, J., Miesel, J., 2019. Soil carbon pools and fluxes vary across a burn severity gradient three years after wildfire in Sierra Nevada mixed-conifer forest. Geoderma 333, 10–22.
Alcañiz, M., Outeiro, L., Francos, M., Ubeda, X., 2018. Effects of prescribed fires on soil properties: a review. Sci. Total Environ. 613–614, 944–957.
Anderson, L., 2011. Holocene record of precipitation seasonality from lake calcite δ18O in the central Rocky Mountains, United States. Geology 39, 211–214.
Binford, M.W., 1990. Calculation and uncertainty analysis of Pb-210 dates for PIRLA project lake sediment cores. J. Paleolimnol. 3, 253–267.
Box, J.E., Colgan, W.T., Christensen, T.R., Schmidt, N.M., Lund, M., Parmentier, F.-J.W., Brown, R., Bhatt, U.S., Euskirchen, E.S., Romanovsky, V.E., Walsh, J.E., Overland, J.E., Wang, M., Corell, R.W., Meier, W.N., Wouters, B., Mernild, S.,

Mård, J., Pawlak, J., Olsen, M.S., 2019. Key indicators of Arctic climate change: 1971–2017. Environ. Res. Lett. 14.
Bracken, M.E.S., Hillebrand, H., Borer, E.T., Seabloom, E.W., Cebrian, J., Cleland, E.E., Elser, J.J., Gruner, D.S., Harpole, W.S., Ngai, J.T., Smith, J.E., 2015. Signatures of nutrient limitation and co-limitation: responses of autotroph internal nutrient concentrations to nitrogen and phosphorus additions. Oikos 124, 113–121.
Briggs, J.C., Ficke, J.F., 1977. In: Interior, D.o.t. (Ed.), Quality of Rivers of the United States, 1975 Water Year - Based on the National Stream Quality Accounting Network (NASQAN). U.S. Geological Survey, Reston, Virginia.
Cade-Menun, B.J., Berch, S.M., Preston, C.M., Lavkulich, L.M., 2000. Phosphorus forms and related soil chemistry of Podzolic soils on northern Vancouver Island. II. The effects of clear-cutting and burning. Can. J. For. Res. 30, 1726–1741.
Calder, W.J., Parker, D., Stopka, C.J., Jimenez-Moreno, G., Shuman, B.N., 2015. Medieval warming initiated exceptionally large wildfire outbreaks in the Rocky Mountains. Proc. Natl. Acad. Sci. U.S.A. 112, 13261–13266.
Calder, W.J., Shuman, B., 2017. Extensive wildfires, climate change, and an abrupt state change in subalpine ribbon forests, Colorado. Ecology 98, 2585–2600.
Calder, W.J., Stefanova, I., Shuman, B., 2018. Climate-fire-vegetation interactions and the rise of novel landscape patterns in subalpine ecosystems, Colorado. J. Ecol. 107, 1689–1703.
Carter, V.A., Power, M.J., Lundeen, Z.J., Morris, J.L., Petersen, K.L., Brunelle, A., Anderson, R.S., Shinker, J.J., Turney, L., Koll, R., Bartlein, P.J., 2018. A 1,500-year synthesis of wildfire activity stratified by elevation from the U.S. Rocky Mountains. Quat. Int. 488, 107–119.
Certini, G., 2005. Effects of fire on properties of forest soils: a review. Oecologia 143, 1–10.
Chapin, F.S., Woodwell, G.M., Randerson, J.T., Rastetter, E.B., Lovett, G.M., Baldocchi, D.D., Clark, D.A., Harmon, M.E., Schimel, D.S., Valentini, R., Wirth, C., Aber, J.D., Cole, J.J., Goulden, M.L., Harden, J.W., Heimann, M., Howarth, R.W., Matson, P.A., McGuire, A.D., Melillo, J.M., Mooney, H.A., Neff, J.C., Houghton, R.A., Pace, M.L., Ryan, M.G., Running, S.W., Sala, O.E., Schlesinger, W.H., Schulze, E.D., 2006. Reconciling carbon-cycle concepts, terminology, and methods. Ecosystems 9, 1041–1050.
Clark, J.S., 1988. Particle motion and the theory of charcoal analysis: source area, transport, deposition, and sampling. Quat. Res. 30, 67–80.
Cook, E., Seager, R., Cane, M., Stahle, D., 2007. North American drought: reconstructions, causes, and consequences. Earth Sci. Rev. 93–134.
Dunnette, P.V., Higuera, P.E., McLauchlan, K.K., Derr, K.M., Briles, C.E., Keefe, M.H., 2014. Biogeochemical impacts of wildfires over four millennia in a Rocky Mountain subalpine watershed. New Phytol. 203, 900–912.
Dzwonko, Z., Loster, S., Gawroński, S., 2015. Impact of fire severity on soil properties and the development of tree and shrub species in a Scots pine moist forest site in southern Poland. For. Ecol. Manag. 342, 56–63.
Elliott, E.M., Brush, G.S., 2006. Sedimented organic nitrogen isotopes in freshwater wetlands record long-term changes in watershed nitrogen source and land usesotopes in freshwater wetlands. Environ. Sci. Technol. 40, 2910–2916.
Filippelli, G.M., Souch, C., Horn, S.P., Newkirk, D., 2009. The pre-Colombian footprint on terrestrial nutrient cycling in Costa Rica: insights from phosphorus in a lake sediment record. J. Paleolimnol. 43, 843–856.
Haliuc, A., Hutchinson, S.M., Florescu, G., Feurdean, A., 2016. The role of fire in landscape dynamics: an example of two sediment records from the Rodna Mountains, northern Romanian Carpathians. Catena 137, 432–440.
Haslett, J., Parnell, A.C., 2008. A simple monotone process with applications to radiocarbon-dated depth chronologies. J. Roy. Stat. Soc. C 57, 399–418.
Higuera, P., Peters, M., Brubaker, L., Gavin, D., 2007. Understanding the origin and analysis of sediment-charcoal records with a simulation model. Quat. Sci. Rev. 26, 1790–1809.
Higuera, P.E., Brubaker, L.B., Anderson, P.M., Hu, F.S., Brown, T.A., 2009. Vegetation mediated the impacts of postglacial climate change on fireregimes in the south-central Brooks Range, Alaska. Ecol. Monogr. 79, 201–219.
Higuera, P.E., Gavin, D.G., Bartlein, P.J., Hallett, D.J., 2010. Peak detection in sediment–charcoal records: impacts of alternative data analysis methods on fire-history interpretations. Int. J. Wildland Fire 19, 996–1014.
Horton, J.D., San Juan, C.A., Stoeser, D.B., 2017. The State Geologic Map Compilation (SGMC) Geodatabase of the Conterminous United States (Ver. 1.1). U.S. Geologiical Survey Data Series 1052, p. 46.
Howe, E., Baker, W.L., 2003. Landscape heterogeneity and disturbance interactions in a subalpine watershed in northern Colorado, USA. Ann. Assoc. Am. Geogr. 93, 797–813.
Hudiburg, T.W., Higuera, P.E., Hicke, J.A., 2017. Fire-regime variability impacts forest carbon dynamics for centuries to millennia. Biogeosciences 14, 3873–3882.
Jiménez-Moreno, G., Anderson, R.S., Shuman, B.N., Yackulic, E., 2019. Forest and lake dynamics in response to temperature, North American monsoon and ENSO variability during the Holocene in Colorado (USA). Quat. Sci. Rev. 211, 59–72.
Johnstone, J.F., Hollingsworth, T.N., Chapin, F.S., Mack, M.C., 2010. Changes in fire regime break the legacy lock on successional trajectories in Alaskan boreal forest. Global Change Biol. 16, 1281–1295.
Kelly, R., Genet, H., McGuire, A.D., Hu, F.S., 2016. Palaeodata-informed modelling of large carbon losses from recent burning of boreal forests. Nat. Clim. Change 6, 79–84.
Leys, B., Higuera, P.E., McLauchlan, K.K., Dunnette, P.V., 2016. Wildfires and geochemical change in a subalpine forest over the past six millennia. Environ. Res. Lett. 11, 125003.
Mack, M.C., Bret-Harte, M.S., Hollingsworth, T.N., Jandt, R.R., Schuur, E.A., Shaver, G.R., Verbyla, D.L., 2011. Carbon loss from an unprecedented Arctic tundra wildfire. Nature 475, 489–492.
Marlon, J.R., Bartlein, P.J., Gavin, D.G., Long, C.J., Anderson, R.S., Briles, C.E., Brown, K.J., Colombaroli, D., Hallett, D.J., Power, M.J., Scharf, E.A., Walsh, M.K., 2012. Long-term perspective on wildfires in the western USA. Proc. Natl. Acad. Sci. Unit. States Am. 109, E535–E543.
McCullough, I.M., Cheruvelil, K.S., Lapierre, J.F., Lottig, N.R., Moritz, M.A., Stachelek, J., Soranno, P.A., 2019. Do lakes feel the burn? Ecological consequences of increasing exposure of lakes to fire in the continental United States. Global Change Biol. 25, 2841–2854.
McLauchlan, K.K., Higuera, P.E., Gavin, D.G., Perakis, S.S., Mack, M.C., Alexander, H., Battles, J., Biondi, F., Buma, B., Colombaroli, D., Enders, S.K., Engstrom, D.R., Hu, F.S., Marlon, J.R., Marshall, J., McGlone, M., Morris, J.L., Nave, L.E., Shuman, B., Smithwick, E.A.H., Urrego, D.H., Wardle, D.A., Williams, C.J., Williams, J.J., 2014. Reconstructing disturbances and their biogeochemical consequences over multiple timescales. Bioscience 64, 105–116.
Meyers, P.A., 1997. Organic geochemical proxies of paleoceanographic, paleolimnologic, and paleoclimatic processes. Org. Geochem. 27, 213–250.
Michelutti, N., Douglas, M.S.V., Wolfe, A.P., Smol, J.P., 2006. Heightened sensitivity of a poorly buffered high arctic lake to late-Holocene climatic change. Quat. Res. 65, 421–430.
Morris, J.L., McLauchlan, K.K., Higuera, P.E., 2015. Sensitivity and complacency of sedimentary biogeochemical records to climate-mediated forest disturbances. Earth Sci. Rev. 148, 121–133.
Parish, M., Calder, W.J., Shuman, B.N., 2020. Millennial-scale increase in winter precipitation in the southern Rocky mountains during the common era. Quat. Res. 1–13.
Parnell, A.C., Haslett, J., Allen, C.M., Buck, C.E., Huntley, B., 2008. A flexible approach to assessing synchroneity of past events using Bayesian reconstructions of sedimentation history. Quat. Sci. Rev. 27, 1872–1885.
Pellegrini, A.F.A., Ahlstrom, A., Hobbie, S.E., Reich, P.B., Nieradzik, L.P., Staver, A.C., Scharenbroch, B.C., Jumpponen, A., Anderegg, W.R.L., Randerson, J.T., Jackson, R.B., 2018. Fire frequency drives decadal changes in soil carbon and nitrogen and ecosystem productivity. Nature 553, 194–198.
Petticrew, E.L., Owens, P.N., Giles, T.R., 2006. Wildfire effects on the quantity and composition of suspended and gravel-stored sediments. Water Air Soil Pollut. Focus 6, 647–656.
Pompeani, D.P., McLauchlan, K.K., Chileen, B.V., Wolf, K.D., Higuera, P.E., 2018. Variation of key elements in soils and plant tissues in subalpine forests of the northern Rocky Mountains, USA. Biogeosci. Discuss. 1–19.
Ray, A.J., Barsugli, J.J., Averty, K.B., Wolter, K., Hoerling, M., Doesken, N., Udall, B., Webb, R.S., 2008. Climate Change in Colorado: a Synthesis to Support Water Resource Management and Adaptation. Colorado Water Conservation Board: CU-Boulder University Communications, Marketing & Creative Services, Boulder, CO.
Reimer, P.J., Bard, E., Bayliss, A., Beck, J.W., Blackwell, P.G., Ramsey, C.B., Buck, C.E., Cheng, H., Edwards, R.L., Friedrich, M., Grootes, P.M., Guilderson, T.P., Haflidason, H., Hajdas, I., Hatte, C., Heaton, T.J., Hoffmann, D.L., Hogg, A.G., Hughen, K., Kaiser, K.F., Kromer, B., Manning, S.W., Niu, M., Reimer, R.W., Richards, D.A., Scott, E.M., Southon, J.R., Staff, R.A., Turney, C.S.M., van der Plicht, J., 2013. IntCal13 and Marine13 Radiocarbon age calibration curves 0-50,000 years cal BP. Radiocarbon 55, 1869–1887.
Rhoades, C.C., Chow, A.T., Covino, T.P., Fegel, T.S., Pierson, D.N., Rhea, A.E., 2018. The legacy of a severe wildfire on stream nitrogen and carbon in headwater catchments. Ecosystems 22, 643–657.
Santin, C., Doerr, S.H., 2016. Fire effects on soils: the human dimension. Philos. Trans. R. Soc. Lond. Ser. B Biol. Sci. 371, 20150171.
Schindler, D.W., Carpenter, S.R., Chapra, S.C., Hecky, R.E., Orihel, D.M., 2016. Reducing phosphorus to curb lake eutrophication is a success. Environ. Sci. Technol. 50, 8923–8929.
Schlesinger, W.H., Dietze, M.C., Jackson, R.B., Phillips, R.P., Rhoades, C.C., Rustad, L.E., Vose, J.M., 2016. Forest biogeochemistry in response to drought. Global Change Biol. 22, 2318–2328.
Shuman, B., Henderson, A.K., Colman, S.M., Stone, J.R., Fritz, S.C., Stevens, L.R., Power, M.J., Whitlock, C., 2009. Holocene lake-level trends in the Rocky mountains, USA. Quat. Sci. Rev. 28, 1861–1879.
Shuman, B.N., Routson, C., McKay, N., Fritz, S., Kaufman, D., Kirby, M.E., Nolan, C., Pederson, G.T., St-Jacques, J.-M., 2018. Placing the Common Era in a Holocene context: millennial to centennial patterns and trends in the hydroclimate of North America over the past 2000 years. Clim. Past 14, 665–686.
Smithwick, E.A.H., 2011. Pyrogeography and biogeochemical resilience. In: McKenzie, D., Miller, C., Falk, D. (Eds.), The Landscape Ecology of Fire. Ecological Studies (Analysis and Synthesis). Springer, Dordrecht.
Smithwick, E.A.H., Kashian, D.M., Ryan, M.G., Turner, M.G., 2009. Long-term nitrogen storage and soil nitrogen availability in post-fire lodgepole pine ecosystems. Ecosystems 12, 792–806.
Smithwick, E.A.H., Turner, M.G., Mack, M.C., Chapin, F.S., 2005. Postfire soil N cycling in northern conifer forests affected by severe, stand-replacing wildfires. Ecosystems 8, 163–181.
Snyder, G.L., 1978. In: Interior, U.S.D.o.t. (Ed.), Intrusive Rocks Northeast of Steamboat Springs, Park Range, Colorado. U.S. Geological Survey, Washington D.C.
Spencer, C.N., Gabel, K.O., Hauer, F.R., 2003. Wildfire effects on stream food webs and nutrient dynamics in Glacier National Park, USA. For. Ecol. Manag. 178, 141–153.
Turner, M.G., Braziunas, K.H., Hansen, W.D., Harvey, B.J., 2019a. Short-interval severe fire erodes the resilience of subalpine lodgepole pine forests. Proc. Natl.

Acad. Sci. U.S.A. 116, 11319–11328.
Turner, M.G., Whitby, T.G., Romme, W.H., 2019b. Feast not famine: nitrogen pools recover rapidly in 25-yr old postfire lodgepole pine. Ecology 100, e02626.
Vieira, D.C.S., Malvar, M.C., Martins, M.A.S., Serpa, D., Keizer, J.J., 2018. Key factors controlling the post-fire hydrological and erosive response at micro-plot scale in a recently burned Mediterranean forest. Geomorphology 319, 161–173.
Walker, X.J., Baltzer, J.L., Cumming, S.G., Day, N.J., Ebert, C., Goetz, S., Johnstone, J.F., Potter, S., Rogers, B.M., Schuur, E.A.G., Turetsky, M.R., Mack, M.C., 2019. Increasing wildfires threaten historic carbon sink of boreal forest soils. Nature 572, 520–523.
Westerling, A.L., 2016. Increasing western US forest wildfire activity: sensitivity to changes in the timing of spring. Philos. Trans. R. Soc. Lond. Ser. B Biol. Sci. 371, 20150178.
Whitlock, C., Anderson, R.S., 2003. Fire history reconstructions based on sediment records from lakes and wetlands. In: Veblen, T.T., Baker, W.L., Montenegro, G., Swetnam, T.W. (Eds.), Fire and Climatic Change in Temperate Ecosystems of the Western Americas. Springer Publishing.
Yelenik, S., Perakis, S., Hibbs, D., 2013. Regional constraints to biological nitrogen fixation in post-fire forest communities. Ecology 94, 739–750.